RSC Advances

ROYAL SOCIETY OF CHEMISTRY

www.rsc.org/advances

Polymerization Mechanism of Poly(Ethylene Glycol Dimethacrylate) Fragrance Nanocapsules

Di Zhao,[1] Xin Jiao,[1] Yao Zhang,[1] Dong An,[1] Xiaodi Shi,[1] Xihua Lu, [1,2*] Gao Qiu,[2] Kenneth J. Shea[3]

[1]College of Chemistry, Chemical Engineering and Biotechnology Donghua University, Shanghai 201620, People's Republic of China

[2]State Key Laboratory for Modification of Chemical Fibers and Polymer Materials, College of Materials Science and Engineering, Shanghai 201620, People's Republic of China

[3]Department of Chemistry, University of California, Irvine, CA 92697, USA

Corresponding author: E-mail Address: xhlu2002@gmail.com. Tel: +862167792776. Fax: +86216779 2776

ABSTRACT

In this paper, a pseudo-ternary phase diagram was drawn according to the phase separation theory to decide if O/W capsules can be formed by using poly(ethylene glycol dimethacrylate) as shell material and fragrance dementholized peppermint oil as model core material. Within a certain ratio range of reaction reagent, the nanocapsule was first synthesized by the precipitation of crosslinking agent on the surface of nanoemulsion. The encapsulation efficiency of dementholized peppermint oil in nanocapsules was above 86.3 %, the average diameter was 261 nm, the particle size distribution was 0.195 and the final conversion rate of ethylene glycol dimethacrylate reached up to 92 %. It was also demonstrated that the nanocapsules' sizes can be tuned by carbon numbers of polyol dimethyl acrylates.

Key words: Poly(ethylene glycol dimethacrylate), crosslinking agent, nanocapsules, phase separation , pseudo-ternary phase diagram.

1. Introduction

With the increase in demand for high quality of life, fragrances are becoming more

and more important in everyday life [1-4]. However, the main ingredients of fragrances are labile and volatile. Therefore a variety of technologies have been developed to improve the storage stability of fragrance materials, including the use of inert atmosphere technique, adding into fixative (benzoin resin), decreasing storage temperature and encapsulation technique [5].

Encapsulation is the most widely used method to protect the fragrances from volatization because encapsulation can improve the physical property (such as colour, appearance, solubility) of core materials, increase the stability of core materials from the environment, prolong the storage time, decrease the harmful effect of toxic substances and control the release of core materials [6-11]. Capsules consist of an active core material in any physical state surrounded by one layer or multilayers of a polymeric membrane ranging in size from several nanometers to micrometers.

Compared to microcapsules, nanocapsules have their own advantages, for example, they have a strong target property [12-15]. Because of nanocapsules' small size, they can be used in intravenous infusion [16, 17]. Meanwhile, they can disperse in water easily forming transparent or translucent colloidal solution. Relatively small size of nanocapsule was expected to resist the frictional destruction of the particles, which is frequently observed in case of microcapsules. Sung Ok Sohn et al. found that nanocapsules showed slower and more stable releasing profile which was under two thirds of that with microcapsules [18]. At present, most nanocapsules were prepared by monomers and crosslinking agents, such as melamine-formaldehyde, polyurethane, polyester and acrylic resin polymers [19, 20], but many residues in the synthetic process are toxic including toluene diisocynate (TDI), formaldehyde, glutaraldehyde, which greatly limit the application of nanocapsules. In this case, it is significant to explore nontoxic material for preparation.

The PEG alone is bio-inert and PEGDM derivatives are biocompatible [21]. Feng Hailiang et al. synthesized P(EGDMA-co-MAA)/PDVB hybrid nanocapsules by using EGDMA as crosslinking agent [22]. Du Pengcheng et al. prepared P(MAA-co-EGDMA) nanocapsules to load the drug doxorubicin for tumor therapy [23]. Abbas Rezaee Shirin-Abadi et al. encapsulated n-hexadecane with PMMA shell

and EGDMA crosslinking agent [24]. In this paper, nanocapsules were prepared only by the crosslinking agent — ethylene glycol dimethacrylate (EGDMA) for it has two double bonds and its polymer chains can crosslink with each other to form a three-dimensional network structure. Phase separation principle was used to explain the possibility of the formation of core-shell structure and the pseudo-ternary phase diagram was drawn to predict the conditions to form the O/W capsules. It was found that in a certain ratio range of water, core material and surfactant, the O/W capsules can be formed and the reaction mechanism of miniemulsion polymerization has been studied by infrared spectroscopy. Nanocapsules with poly(ethylene glycol dimethacrylate) (PEGDMA) shell possess desirable properties of hydrogel [25, 26], nontoxicity, and excellent biocompatibility.

2. Experimental methods

2.1 Materials

Ethylene glycol dimethacrylate (EGDMA, Aldrich, 99%, 198.22 g/mol), 1,4-butandiol dimethacrylate (BDDMA, Aldrich, 99%, 226.27 g/mol), and 1,6-hexandiol dimethacrylate (HDDMA, Aladdin, 99%, 254.32 g/mol) were used as received without further purification. Benzoyl peroxide (BPO, Aldrich, 75%, 242.23 g/mol), hexadecane (HD, Ourchem, 99%, 226.44 g/mol), and mowiol®4-88 (M-4-88, Aldrich, 88 % hydrolysis degree of polyvinyl alcohol, 31000 g/mol) were used as received. The dementholized peppermint oil (DPO, CP) was provided by Anhui Fengle Perfume and used without further purification. Ultrapure water was used for all experiments.

2.2 Preparation of nanocapsules

Nanocapsules were prepared by a “polymer precipitation” method. First, M-4-88 was dissolved in water (below its critical micelle concentration) to prepare the aqueous phase. Then, BPO, HD and EGDMA were dissolved in DPO at RT to prepare the oil phase. The resulting oil solution was poured into the aqueous phase and emulsified with an ultrasound device SCIENTZ®JY92-IIDN for 30 min resulting in forming of nanoemulsion (NE) which was refered to the emulsion before

polymerization. Heating the emulsion at 80 ℃ under gentle stirring allowed the BPO to trigger the polymerization under the protection of N_2 forming nanocapsule (NC) which was after the polymerization.

2.3 Dynamic light scattering (DLS) characterization

The size and size distribution of NC were determined by DLS with a BI-9000 AT digital time correlator (BI-200SM, Brookhaven Co. Ltd.) in the condition of 90° for scattering angle. Light source is a He-Ne laser with 35 mW and 633 nm.

2.4 Field Emission Scanning Electron Microscope (FE-SEM)

FE-SEM was performed with a Hitachi®S-4800 microscope. Thereby an accelerating voltage of 0.5~30 KV was used.

2.5 Transmission electron microscopy (TEM)

TEM was performed with a Hitachi CO. H-800 at an accelerating voltage of 200 KV and the samples were prepared by placing a dilute drop of the measured solution onto the copper grids and allowing it to dry.

2.6 UV-vis spectrophotometer characterization

Fragrance loading efficiency was determined by means of UV-visible spectrophotometer (PerkinElmer, USA) at the wavelength of 283 nm.

2.7 Pyrolysis gas chromatography-mass spectrometry (PyGC-MS)

The residual content of reaction monomer was measured by means of PyGC-MS with a Shimadzu®QP-2010Ultra instrument.

2.8 Large Surface Analyzer (LSA)

LSA was performed with a Krüss®DSA-30 analyzer to measure the contact angle between a liquid and a solid.

2.9 Fourier transform infrared (FTIR) spectroscopy

FT-IR was performed with a Thermo Fisher®Nicolet iN 10 MX microscope running at a 4 cm^{-1} resolution.

2.10 Thermal gravimetric analysis (TGA)

The thermal stabilities of DPO, NC and PEGDMA shell material with increasing temperature were evaluated by the thermal gravimetric analysis (TGA, TG209F1, German resistance instrument co.,Ltd) under an atmosphere of N_2 from 50 °C to

600 °C at a heating rate of 10 °C/min.

3. Results and Discussion

3.1 The theory of phase separation

Table 1. Values of γ, γ^d and γ^h

	water	DPO	PEGDMA
γ (mNm^{-1})	72.8	26.9	36.1
γ^d (mNm^{-1})	21.8	20.8	15.4
γ^h (mNm^{-1})	51.0	6.1	20.7

The phase separation theory of Torza and Mason [27] was used to predict whether the core-shell structure can be formed or not by characterizing the spreading coefficient S. In this experiment, DPO was phase 1, water was phase 2 and PEGDMA was phase 3.

Then the interfacial tension γ, γ^d and γ^h ($\gamma = \gamma^d + \gamma^h$. γ represents the interfacial tension between two insoluble phase. γ^d and γ^h represent the dispersion force and the hydrogen bond force, respectively) of the substances involved in the experiment under 20 ℃ can be calculated and showed in **Table 1**. From the results in **Table 1**, values of spreading coefficient S_1, S_2 and S_3 can be calculated below.

$$S_1 = \gamma_{23} - (\gamma_{12} + \gamma_{13}) = -19.30 \text{ mN/m} < 0$$

$$S_2 = \gamma_{13} - (\gamma_{12} + \gamma_{23}) = -24.36 \text{ mN/m} < 0$$

$$S_3 = \gamma_{12} - (\gamma_{13} + \gamma_{23}) = 9.82 \text{ mN/m} > 0$$

Because $S1 < 0$, $S2 < 0$, $S3 > 0$, a core-shell structure can be formed by using PEGDMA as shell material and DPO as core material.

3.2 Pseudo-ternary phase diagram

In order to obtain stable O/W NC, the ratio of oil, surfactant and aqueous solution (ultrapure water) was in a certain range [28]. Then pseudo-ternary systems with various weight ratios of oil (DPO), surfactant (M-4-88) and aqueous solution (ultrapure water) were prepared and left overnight to equilibrate. Dilution and visual observation were used to identify the result of the combinations. When the O/W nanocapsule can be formed under a certain ratio, the ratio represented by a spot was marked in the pseudo-ternary phase diagram. Finally, the left region drawn by these spots in

approximate triangle was the O/W nanocapsule (NC) (**Fig.1**).

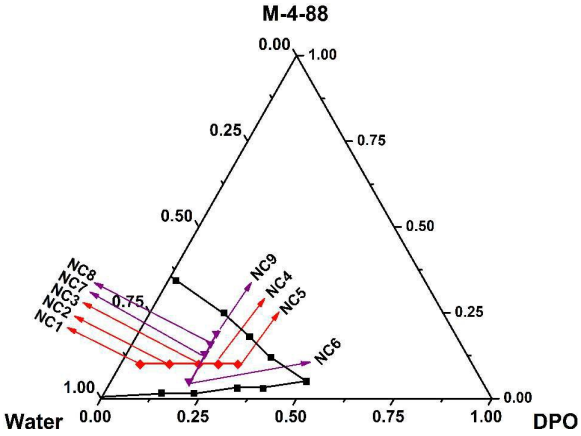

Figure1. Pseudo-ternary phase diagram

3.3 A typical recipe of nanocapsule

To testify the validity of the Pseudo-ternary phase diagram, NC3 (**Table 2)** was taken as an example. The encapsulation efficiency was 86.3 % measured by UV-visible spectrophotometer (**Figure S1**), the average diameter of the final NC was 261 nm and the particle size distribution was 0.195 measured by DLS (**Figure S3**). The capsules of core-shell structures can be formed as shown in TEM image (**Fig.2**) below. And the thickness of the shell was 20-50 nm which confirmed that the O/W capsules can be formed by using PEGDMA as shell material and DPO as core material.

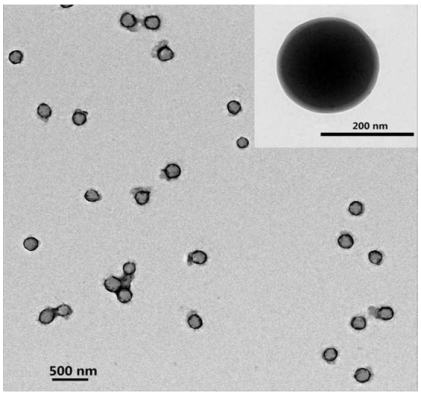

Figure2. Transmission electron micrograph of NC

3.4 Different compositions of nanocapsules

Fig.3 showed the influence of DPO and surfactant on the NC radius. The different compositions of NC (**Table 2**) were shown by the nine points in **Fig.1**. The series of

NC1→NC2→NC3→NC4→NC5 was an increase of DPO indicating when the dosage of EGDMA, BPO and surfactant was fixed, the radius of the NC droplets increased with an increase of DPO (**Fig.3 (a)**). And the series of NC6→NC3→NC7→NC8→NC9 was an increase of surfactant indicating when the dosage of EGDMA, BPO and DPO was fixed, the radius of the NC droplets decreased with an increase of surfactant concentration (**Fig.3 (b)**) [29].

Table 2. Different compositions of nanocapsules

	NC1	NC2	NC3	NC4	NC5	NC6	NC7	NC8	NC9
DPO [wt %]	5	12	19	24	29	19	19	19	19
Surfactant [wt %]	1	1	1	1	1	0.5	1.3	1.6	1.8
BPO [wt %]	0.1	0.1	0.1	0.1	0.1	0.1	0.1	0.1	0.1
EGDMA [wt %]	3	3	3	3	3	3	3	3	3

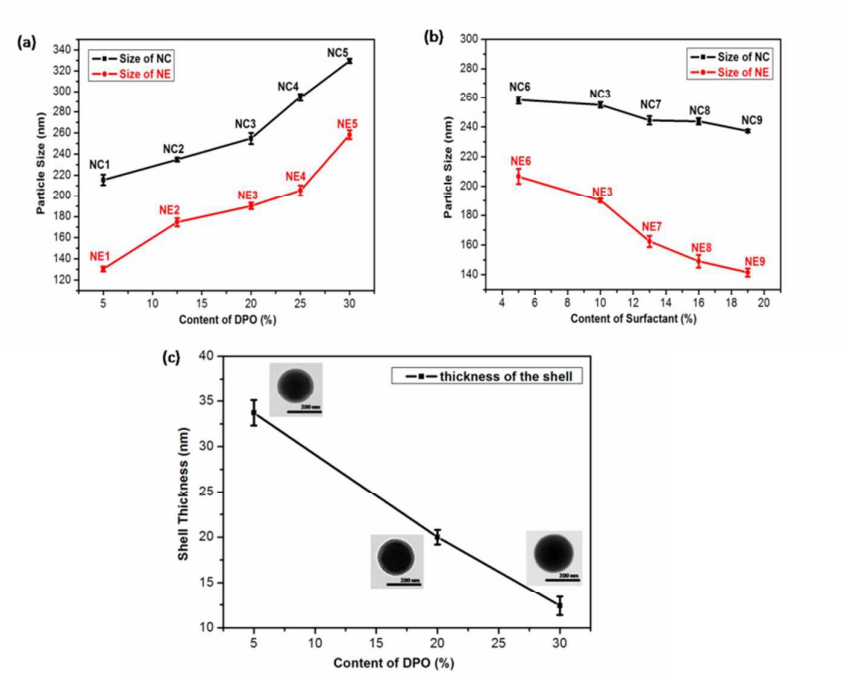

Figure3. Effects of (a) DPO and (b) surfactant content on the size of NE and NC; Effects of (c) DPO on the thickness of NC, the scale bar was 200 nm

At the same time, the size change of NE was in consistent with the change of NC size (**Fig.3**). That showed the polymerization of EGDMA in NE happened just on the surface of the droplets of NE. The original NE acted as the template in the NC

preparation. Furthermore, it was very interesting to see the decrease in the shell thickness from 33.7 nm to 12.4 nm with the increase of DPO content from 5 % to 30 % as shown in **Fig.3 (c).** The reason for this might be the decrease of ratio between monomer and DPO when the content of monomer was fixed and the content of DPO was increased. Therefore, there was less monomer in each nanodrop to form the shell leading a decrease of shell thickness.

The long time stability is of major importance for these fragrance nanocapsules. The particle diameters of NE3 and NC3 were measured by DLS against storage time at two temperatures, 15 ℃ and 50 ℃, to characterize their stability. The NC3 was very stable during the studied elapse time of 60 days as shown in **Fig.4 (a)**. On the contrary, the NE3 was very unstable (**Fig.4 (a)**) with a significant change in size. Ostwald ripening was the most likely reason to explain the unstability of NE. Ostwald ripening of emulsion was fast, which caused the bigger O/W droplets of the size distribution to increase and the smaller to shrink. In any case, the stability of the NE is enough for allowing the formation of shell with good stability since the polymerization quickly took place in a few minutes. Therefore, once the shell formed, the Ostwald ripening will be removed [30]. The stability results in **Fig.4 (a)** showed the shell can protect core material from leaking into water phase.

The thermal stabilities of the DPO, the NC and PEGDMA shell material under nitrogen were evaluated by thermo gravimetric analysis (TGA) from 50 °C to 600 °C shown in **Fig.4 (b)**. The degradation region of the PEGDMA shell material was from 320 °C to 450 °C. According to the TGA curve of DPO, the onset evaporation temperature of DPO was 50 °C. As DPO was encapsulated by the PEGDMA shell, the onset evaporation temperature of DPO was increased to 150 °C. This demonstrated that the nanocapsule can improve the onset evaporation temperature of DPO and increase the usage temperature region of DPO. In other words, the PEGDMA nanocapsules had a good thermal stability and can control the release of DPO.

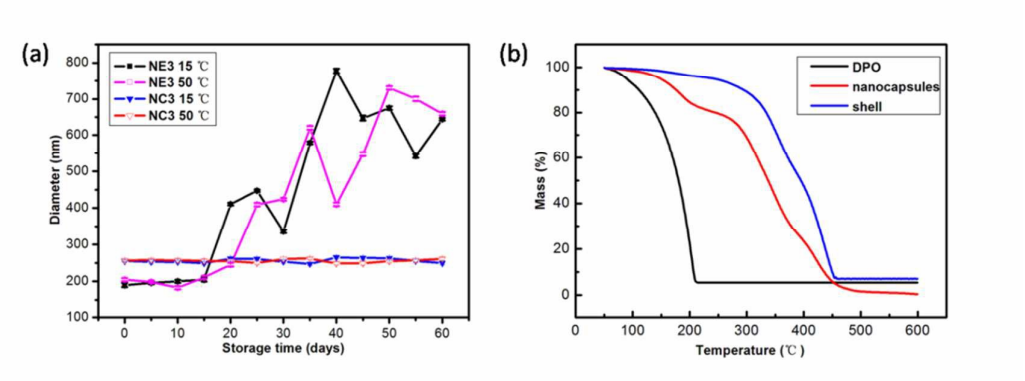

Figure4. (a) Size of NE3 and NC3 at 15 ℃ and 50 ℃;

(b) TGA of DPO, nanocapsules and PEGDMA shell materials

Meanwhile, NE3 was taken as an example to investigate the dynamical features of miniemulsion polymerization. In the process of polymerization, samples were taken every 30 minutes to measure residual content of EGDMA by PyGC-MS. Then, the relationship between the conversion of EGDMA and time was showed in **Fig.5 (a)**, and the rate of polymerization was showed in **Fig.5 (b)**.

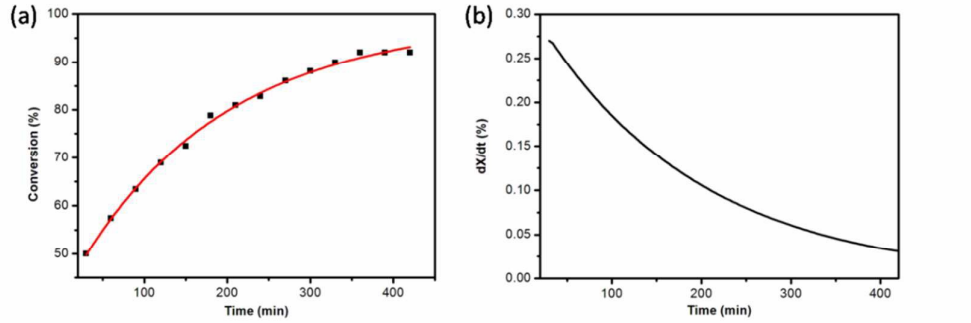

Figure5. (a) Conversion-time curve and (b) Polymerization rate-time curve

With the polymerization going on, the free radicals in the NC were approaching to equilibrium. Most of the monomers have been polymerized leading to the decrease of monomers which were inside the NC. Therefore, the rate of polymerization declined gradually to a constant. The results showed about 92 % of EGDMA has been polymerized finally indicating the monomer had a high utilization rate during the reaction.

3.5 Mechanism of nanocapsule formation

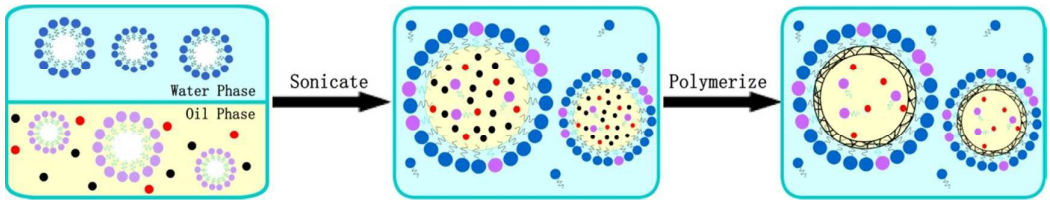

Figure6. Preparation of nanocapsules by miniemulsion polymerization,

: Emulsifer; : Costabilizer; :Initiator; :Monomer; :PEGDMA network

Different from the nucleation mechanism by micelles in traditional polymerization, the nucleation mechanism of miniemulsion polymerization is in the nanodrops. After sonication, the O/W nanoemulsion was formed. When the temperature reached 80 ℃, the initiator BPO split into free radicals in the core under the protection of N_2. Then the free radicals activated the carbon-carbon double bond of EGDMA towards radical addition resulting in the increase of chains to form the oligomer at the oil-water interface. As the decrease of EGDMA at the interface, the EGDMA in the internal nanodrops migrated to the interface to continue the polymerization. Afterwards, oligomer was further triggered by free radicals leading to the growth of chains. Finally, chain aggregation with each other formed the PEGDMA network. Based on the data of the spreading coefficient S_1, S2 and S_3 in 3.1, the PEGDMA network separated from the oil phase and deposited onto the surface of existing NE particles. Then PEGDMA nanocapsules were synthesized due to PEGDMA precipitation on the surface of NE (**Fig.6**) [31-34].

In the study, infrared spectra (**Fig.7**) was used to characterize the structure of the NC. The monomer EGDMA consisted of molecule group of $CH_2=CR_1R_2$ whose peak could be identified at 1638 cm^{-1} due to stretching vibration. The rate of the peak intensities between 1638 cm^{-1} and 1729 cm^{-1} (carbonyl group) was 23/87 as shown in **Fig.7 (a)**. When the free radical polymerization of EGDMA finished, most of the EGDMA monomer participated into the polymerization to form the shell because the rate of the peak intensities between 1638 cm^{-1} and 1729 cm^{-1} was 3/88 as shown in **Fig.7 (b)** and 2/88 in the nanocapsules (**Fig.7 (c)**). The decreasing ratio of two peaks of 1638 cm^{-1} and 1729 cm^{-1} of the nanocapsules qualitatively indicated the EGDMA had taken part in the reaction. The crosslinking efficiency was 92 % which was

quantitatively determined by PyGC-MS as shown in **Fig.5**. The peak at 3383 cm^{-1} represented the stretching vibration of hydrogen bond (O-H) in the DPO as shown in **Fig.7 (d)**, which was also observable in the NC spectrum (**Fig.7 (c)**) and disappeared in the shell spectrum (**Fig.7 (b)**). This proved that the nanocapsules contained the DPO. In conclusion, the PEGDMA shell materials synthesized by EGDMA did successfully packet DPO and the NC were formed.

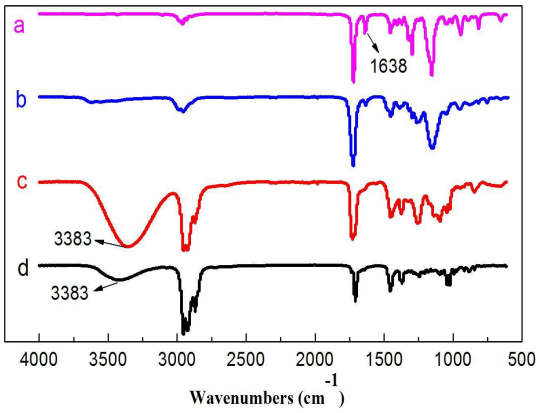

Figure7. Infrared spectra of (a) EGDMA, (b) shell, (c) nanocapsules and (d) DPO

To investigate the formation of NC synthesized with other polyol dimethyl acrylates, 1,4-butandiol dimethacrylate (BDDMA) and 1,6-hexandiol dimethacrylate (HDDMA) were chosed to form NC with the same method (**Figure S2**). DLS results showed with the increase carbon numbers of monomers, the average sizes of NC decreased from 261 nm to 73 nm (**Figure S3**), indicating that the size of NC can be tuned by carbon numbers of monomers. Monomers with more carbon numbers could have faster rate of diffusion in solvent and then quickly form high molecular weight polymer. So the rate of polymerization increased with increasing the carbon numbers of the monomers in this system. When the rate of polymerization increased, the concentration of oligomer decreased. Shouldice et al reported that the low concentration of resulting oligomer at the early stage of the polymerization could lead to the decreasing size of the particles because oligomers are known to be very effective swelling agents[35]. This could explain that the average sizes of NC decreased with increasing carbon numbers of monomers.

4. Conclusions

Phase separation principle and pseudo-ternary phase diagram were applied to predict that dementholized peppermint oil can be encapsuled by poly(ethylene glycol dimethacrylate). The results showed that the average size of nanocapsules was related to the size of primary emulsion and the dosage of core material and surfactant. Meanwhile, the polymerization happened just on the surface of the NE droplets. The ethylene glycol dimethacrylate (EGDMA), a widely used biocompatible cross-linking agent in polymerization [22-26], was employed as the only reactive monomer for encapsulation in this paper. The nanocapsules had a high encapsulation efficiency of 87 %, a low particle-size distribution of 0.195 and a high monomer conversion rate of 92 %. Further, the nanocapsules' sizes can be tuned by carbon numbers of polyol dimethyl acrylates.

The fragrance nanocapsules with poly(ethylene glycol dimethacrylate) as shell material are appropriate for food industry, medicine, textiles and cosmetics. Also, our nanoencapsulation approach is principally not restricted to fragrance and expected to work in conjunction with other hydrophobic substances.

Acknowledgments

The authors thank for financial supports by Science and Technology Commission of Shanghai Municipality (13520720100), National Natural Science Foundation of China (51473032), and National Scientific Foundation (DMR-1308363).

References

1. D.-D. Yin, R.-Y. Yuan, Q. Wu, S.-S. Li, S. Shao, Y.-J. Xu, X.-H. Hao and L.-S. Wang, Food chem., 2015, 187, 20-28.
2. J. Hu, W. J. Deng, L. Q. Liu and Z. B. Xiao, J. Appl. Polym. Sci., 2014, 131.
3. D. Kalemba and A. Kunicka, Curr. Med. Chem., 2003, 10, 813-829.
4. L. Yuan, W. Hongmei, Z. Dapeng and L. Dan, Adv. Mater. Res., 2011, 239-242, 624-627.
5. I. Hofmeister, K. Landfester and A. Taden, Macromolecules, 2014, 47, 5768-5773.
6. D. C. Wan, S. Ohta, T. Kakuchi and T. Satoh, Soft Matter, 2011, 7, 6422-6425.
7. U. Bazylinska, R. Skrzela, K. Szczepanowicz, P. Warszynski and K. A. Wilk,

Soft Matter, 2011, 7, 6113-6124.

8. C. P. Oliveira, C. G. Venturini, B. Donida, F. S. Poletto, I. S. Guterres and A. R. Pohlmann, Soft Matter, 2013, 9, 1141-1150.
9. A. P. Esser-Kahn, S. A. Odom, N. R. Sottos, S. R. White and J. S. Moore, Macromolecules, 2011, 44, 5539-5553.
10. C. Conte, G. Costabile, I. d'Angelo, M. Pannico, P. Musto, G. Grassia, A. Ialenti, P. Tirino, A. Miro, F. Ungaro and F. Quaglia, J. Colloid Interface Sci., 2015, 454, 112-120.
11. F. Cuomo, F. Lopez, M. Piludu, M. G. Miguel, B. Lindman and A. Ceglie, J. Colloid Interface Sci., 2015, 447, 211-216.
12. F. J. Hernandez, L. I. Hernandez, M. Kavruk, Y. M. Arica, G. Bayramoglu, B. A. Borsa, H. A. Oktem, T. Schafer and V. C. Ozalp, Chem. Commun., 2014, 50, 9489-9492.
13. R. I. El-Gogary, N. Rubio, J. T. W. Wang, W. T. Al-Jamal, M. Bourgognon, H. Kafa, M. Naeem, R. Klippstein, V. Abbate, F. Leroux, S. Bals, G. Van Tendeloo, A. O. Kamel, G. A. S. Awad, N. D. Mortada and K. T. Al-Jamal, Acs Nano., 2014, 8, 1384-1401.
14. Y. Nishimura, H. Mieda, J. Ishii, C. Ogino, T. Fujiwara and A. Kondo, J. Nanobiotechnol., 2013, 11.
15. X. Y. Xu, W. Ho, X. Q. Zhang, N. Bertrand and O. Farokhzad, Trends Mol. Med., 2015, 21, 223-232.
16. E. Moysan, Y. Gonzalez-Fernandez, N. Lautram, J. Bejaud, G. Bastiat and J. P. Benoit, Soft Matter, 2014, 10, 1767-1777.
17. D. S. Jornada, L. A. Fiel, K. Bueno, J. F. Gerent, C. L. Petzhold, R. C. R. Beck, S. S. Guterres and A. R. Pohlmann, Soft Matter, 2012, 8, 6646-6655.
18. S. O. Sohn, S. M. Lee, Y. M. Kim, J. H. Yeum, J. H. Choi and H. D. Ghim, Fibers Polym., 2007, 8, 163-167.
19. Y. Liu, Y.Y. Wei, C.Z. Zong, Colloid Polym. Sci., 2014, 292, 873-884.
20. F. Khakzad, Z. Alinejad, A. R. Shirin-Abadi, M. Ghasemi and A. R. Mahdavian, Colloid Polym. Sci., 2014, 292, 355-368.

21. B. K. Mann, A. S. Gobin, A. T. Tsai, R. H. Schmedlen and J. L. West, Biomaterials, 2001, 22, 3045-3051.

22. H.L. Feng, E. Yan, J. Zhang, X.L. Yang, C.X. Li, Polym., 2013, 54, 4511-4520.

23. P. C. Du, H. Y. Yang, J. Zeng and P. Liu, J. Mater. Chem. B., 2013, 1, 5298-5308.

24. A. R. Shirin-Abadi, A. R. Mahdavian and S. Khoee, Macromolecules, 2011, 44, 7405-7414.

25. P. Somasundaran, F. Liu, D. Sarkar and C. C. Gryte, J. Cosmet. Sci., 2004, 55, 222-223.

26. R. R. Zhang, R. S. Yao, B. B. Ding, Y. X. Shen, S. W. Shui, L. Wang, Y. Li, X. Z. Yang and W. Tao, Adv. Mater. Sci. Eng., 2014, DOI: 10.1155/2014/169210.

27. S. Torza, S.G. Mason, J. Colloid Interface Sci., 1970, 33, 67-83.

28. Y. Y. Zhu, X. Q. An, S. P. Li and S. Q. Yu, J. Surfactants Deterg., 2009, 12, 305-311.

29. C. Lo, J. S. Zhang, P. Somasundaran and J. W. Lee, J. Colloid Interface Sci., 2012, 376, 173-176.

30. D. Moinard-Checot, Y. Chevalier, S. Briancon, L. Beney and H. Fessi, J. Colloid Interface Sci., 2008, 317, 458-468.

31. J. S. Downey, R. S. Frank, W. H. Li and H. D. H. Stover, Macromolecules, 1999, 32, 2838-2844.

32. T. B. Zou, Z. P. Zhou, J. D. Dai, L. Gao, X. Wei, C. X. Li, W. X. Guan and Y. S. Yan, J. Polym. Res., 2014, 21.

33. W. H. Li and H. D. H. Stover, Macromolecules, 2000, 33, 4354-4360.

34. R. I. Kusuma, C. T. Lin and C. S. Chern, Polym. Int., 2015, 64, 1389-1398.

35. G. T. D. Shouldice, G. A. Vandezande and A. Rudin, Eur. Polym. J., 1994, 30, 179-183.